Science of the Total Environment 672 (2019) 400–409

Contents lists available at ScienceDirect

Science of the Total Environment

journal homepage: www.elsevier.com/locate/scitotenv

Methane flux dynamics in a submerged aquatic vegetation zone in a subtropical lake

Mi Zhang [a,e], Qitao Xiao [c], Zhen Zhang [a], Yunqiu Gao [d], Jiayu Zhao [a], Yini Pu [a], Wei Wang [a], Wei Xiao [a], Shoudong Liu [a], Xuhui Lee [a,b,*]

[a] Yale-NUIST Center on Atmospheric Environment, International Joint Laboratory on Climate and Environment Change (ILCEC), Nanjing University of Information Science and Technology, Nanjing 210044, China
[b] School of Forestry and Environmental Studies, Yale University, New Haven, CT 06511, USA
[c] Key Laboratory of Watershed Geographic Sciences, Nanjing Institute of Geography and Limnology, Chinese Academy of Sciences, Nanjing 210008, China
[d] Hangzhou Chaoteng Energy Technology Co., Ltd, Hangzhou 310051, China
[e] NUIST-Wuxi Research Institute, Wuxi 214105, China

HIGHLIGHTS

- The CH_4 flux is on average higher at night than during the day, although considerable scatter exists in the diurnal pattern.
- Sediment temperature is a dominant driver that determines daily to seasonal variations of the CH_4 flux.
- The CH_4 flux shows a low temperature sensitivity ($Q_{10} = 1.79$) in the submerged aquatic vegetation zone of the lake.
- Carbon loss via CH_4 emission is about 3.5% of the annual net ecosystem production.

GRAPHICAL ABSTRACT

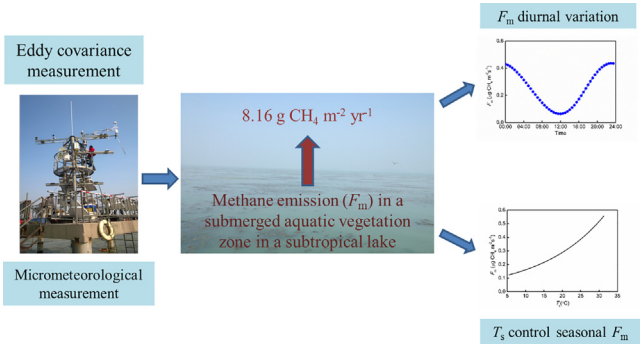

ARTICLE INFO

Article history:
Received 11 December 2018
Received in revised form 26 March 2019
Accepted 30 March 2019
Available online 1 April 2019

Editor: Jay Gan

Keywords:
Methane flux
Submerged aquatic vegetation
Subtropical shallow lake

ABSTRACT

Submerged macrophytes are important primary producers for shallow lake systems. So far, their overall role in regulating lake methane flux is a subject of debate because the oxygen produced by their roots can promote methane oxidation in the sediment but they can also enhance methanogenesis through organic substrate production. In this study, we used the eddy covariance method to investigate the temporal dynamics of the CH_4 flux in a habitat of submerged macrophytes in Lake Taihu. The results show that the nighttime CH_4 flux is on average 33% higher than the daytime flux, although a clear diurnal pattern is evident only in the spring. At the daily to the seasonal time scale, the sediment temperature is the main driver of the CH_4 flux variations, implying higher methane production in the sediment at higher temperatures. The annual CH_4 emission (6.12 g C m^{-2} yr^{-1}) is much higher than the published whole-lake mean flux (1.12 g C m^{-2} yr^{-1}) and that reported previously in the eutrophic phytoplankton zone of the lake (1.35 g C m^{-2} yr^{-1}), indicating that the net effect of the submerged macrophytes is to enhance methane emission. At the annual time scale, 3.5% of the carbon gained by the net ecosystem production is lost to the atmosphere in the form of CH_4.

* Correspondence author at: School of Forestry and Environmental Studies, Yale University, 21 Sachem Street, New Haven, CT 06510, USA.
E-mail address: xuhui.lee@yale.edu (X. Lee).

https://doi.org/10.1016/j.scitotenv.2019.03.466
0048-9697/

1. Introduction

Global lakes are an important natural source of atmospheric methane (Walter et al., 2006, 2007), releasing 72 Tg per year or about 70% of the total freshwater methane emission to the atmosphere (Bastviken et al., 2004 & 2011). Shallow lakes (average depth lower than 3 m), existing in a greater number and occupying a larger area than deep lakes (Downing et al., 2006; Radomski and Perleberg, 2012; Verpoorter et al., 2014; Davidson et al., 2015), are a large contributor to the global lake methane emission (Palma-Silva et al., 2013; Davidson et al., 2015). Submerged macrophytes, plants rooted in the sediment and growing in water, are a common feature of shallow lake systems (Wetzel, 2001; Scheffer, 2004). The role of these aquatic plants in methanogenesis is debatable. Some researchers report that submerged macrophytes inhibit methane emission because oxygen produced by the root of these vascular plants promotes methane oxidation in the sediment (Sorrell et al., 2002; Sorrell and Downes, 2004; Xing et al., 2006). On the other hand, submerged macrophyte may promote methane emission because they provide organic substrate for methanogenesis through their primary production (Xing et al., 2006; Schütz et al., 1991). So far, few long-term (>one year) and continuous measurements are available to quantify the net consequence of these two competing effects (Sorrell et al., 2002; Xing et al., 2006).

The presence of submerged macrophytes may alter the diurnal and seasonal rhythms of the methane flux in relation to meteorological and biological factors. In lake margins and wetlands dominated by emergent vegetation, strong diurnal variations of the CH_4 flux are observed. These variations are characterized by higher fluxes in the daytime and lower fluxes at night, the primary reason being that CH_4 emitting through aerenchyma of vascular plants is a major CH_4 transport pathway (Dalal et al., 2008; Miller, 2011; Knoblauch et al., 2015; Nielsen et al., 2017). However, a different diurnal pattern has been reported, with higher CH_4 fluxes at night and lower fluxes in the daytime, for lake habitats of emergent vegetation (Podgrajsek et al., 2014) and submerged vegetation (Franz et al., 2016), the primary cause being stronger water-side thermal convection at night than during the day. At the seasonal scale, the flux variations are driven by variations in water temperature in lakes with macrophytes (Kankaala et al., 2004; Duan et al., 2005; Franz et al., 2016; Xiao et al., 2017) or without macrophytes (Liu et al., 2017). Because aquatic vegetation grows faster in warmer temperatures, some of the flux seasonal variations in macrophyte-dominated sites may also be contributed by variations in primary production. A precise understanding of the flux temporal variations and their controlling factors can reduce uncertainties in model studies and in field observations aiming to quantify the lake annual methane emission.

Another question regarding aquatic ecosystems is how much of the organic substrate produced by photosynthesis is used to support CH_4 production. Answers to this question are generally expressed as the ratio of the CH_4 emission to the net ecosystem productivity (NEP). In wetlands and rice ecosystems, methane emission increases with increasing NEP, with about 3.3% of the carbon sequestered through NEP lost via methane emission (Whiting and Chanton, 1993). However, in some lakes dominated by aquatic vegetation, the CH_4 emission does not always increase with primary productivity. For example, in a eutrophic shallow lake in the Peene River Valley, Germany, CH_4 emission in the submerged and floating vegetation area is larger than that in the emergent vegetation area, even though the primary production in the submerged and floating vegetation area is lower than that in the emergent vegetation area (Franz et al., 2016). Currently, we lack sufficient field data to constrain the relationship between the methane flux and NEP for lake ecosystems.

Lake Taihu, a large and shallow subtropical lake located in the Yangzi River Delta, China, is an ideal location for investigating the role of submerged macrophytes in lake methane emission. The lake varies spatially in terms of eutrophication status, vegetation type and abundance, and wind-current interactions (Liu et al., 2007; Qin et al., 2007; Lee et al., 2014). The east zone of the lake is dominated by submerged macrophyte, where the highest diffusion methane flux occurs (Xiao et al., 2017). The rest of the lake is open water habitat with varying degrees of eutrophication. A comparative analysis of the flux observed in macrophyte habitats and the flux in other open-water zones will be helpful to determine biotic (phytoplankton versus aquatic vegetation) and abiotic (temperature, wind, turbulent mixing) controls on the methane emission fluxes.

The current study builds on several published observational studies on methane emission in Lake Taihu (Wang et al., 2006; Xiao et al., 2014; Xiao et al., 2017). These published studies either have limited temporal coverage (<30 days, Wang et al., 2006), are restricted to hypereutrophic open-water and littoral zones (Wang et al., 2006; Xiao et al., 2014), or only examine the diffusion component of the methane emission (Xiao et al., 2017). In this study, we deployed the eddy covariance technique to measure the total methane flux (diffusion plus ebullition) at a habitat of submerged macrophytes for three years. In parallel to the eddy covariance measurement was a gradient-diffusion measurement of the total methane flux in the northeastern portion of the lake that was free of aquatic vegetation but experienced heavy algal growth. We aim (1) to examine the temporal dynamics of the CH_4 flux in this macrophyte habitat, (2) to discern meteorological factors that control the diurnal and seasonal variations in the observed CH_4 flux, and (3) to investigate the relationships between the CH_4 flux and the NEP of this aquatic ecosystem.

2. Methods

2.1. Site description

Lake Taihu is a large lake (area 2400 km^2) situated in a humid subtropical climate zone. The annual mean air temperature and annual precipitation are 16.2 °C and 1120 mm, respectively. The lake is divided into seven zones according to pollution status, wind-current interactions, and vegetation type, including a submerged aquatic vegetation zone in the east (Zhao et al., 2011; Liu et al., 2007; Qin et al., 2007; Lee et al., 2014). The flux site (site ID: BFG; 31.14°N, 120.40°E) is located in this zone (Fig. 1). The mean water depth is about 2.1 m. The dominant species are *Hydrilla verticillata* and *Potamogeton malaianus*. The water quality parameters for this zone, including concentration of dissolved organic carbon (DOC), concentration of dissolved oxygen (DO), concentrations of total phosphorus (TP) and total nitrogen (TN), and water clarity, are given in Supplementary Table S1.

2.2. Measurements

The CO_2 flux (F_c) and the CH_4 flux (F_m) between the lake surface and the air were measured by the eddy covariance method,

$$F = \overline{w'c'} \quad (1)$$

where w' is the fluctuating of vertical air velocity, c' is the fluctuating CH_4 or CO_2 density, and the overbar denotes time averaging. The F_c and F_m measurements started at BFG in December 2011 and April 2014, respectively. The data used in this study were collected between May 2014 and May 2017. Two eddy covariance (EC) systems were used, one consisting of a three-dimensional sonic anemometer/thermometer (Model CSAT3, Campbell Scientific Inc., Logan, UT, USA) and an open-path infrared CO_2 and water vapor analyzer (Model EC150, Campbell Scientific Inc., Logan, UT, USA), and the other consisting of a CSAT3 anemometer/thermometer, an EC150 CO_2/H_2O analyzer, and an open-path CH_4 gas analyzer (Model Li-7700, LI-COR Inc., Lincoln, NE, USA). The raw data were collected at 10 Hz and stored by two dataloggers (Model CR3000, Campbell Scientific Inc., Logan, UT, USA), and then were block-averaged over 30-min intervals to calculate the

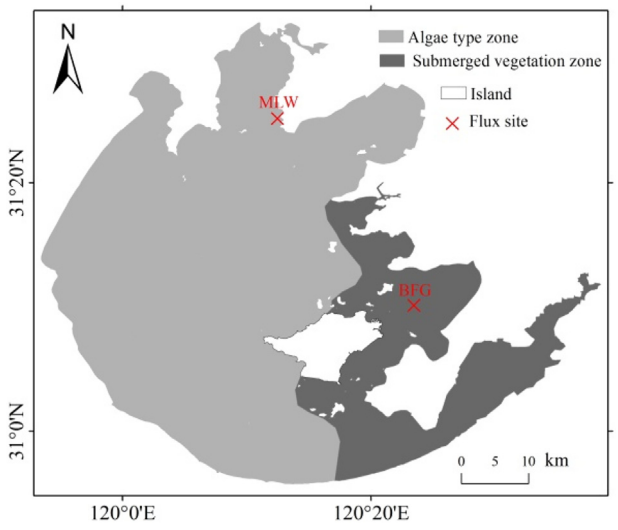

Fig. 1. Map of Lake Taihu showing the location of the eddy covariance site (Bifenggang; BFG) and the flux-gradient site (Meiliangwang; MLW).

CO_2 and CH_4 fluxes. Both EC systems were mounted at a height of 8.5 m above the water surface. The footprint model of Hsieh et al. (2000) predicts that the peak contribution to the EC fluxes is at a distance of about 200 m from the flux tower. The distance between the EC platform and the nearest lake shore is 4 km. Therefore, the EC flux signal was unaffected by land sources and sinks.

In parallel to the EC measurement, air temperature and humidity were measured with a temperature/humidity probe (Model HMP155A; Vaisala, Inc., Helsinki, Finland). Wind speed and wind direction were measured with an anemometer and a wind vane (Model 05103; R M Young Company, Traverse City, Michigan, USA) at the height of 8.5 m above the water surface. Water temperature at the depths of 20, 50, 100, and 150 cm and sediment temperature at the depth of 3 cm below the water column were monitored with temperature probes (Model 109-L, Campbell Scientific Inc., Logan, UT, USA). These meteorological variables were sampled at 1 Hz by a datalogger (Model CR1000, Campbell Scientific Inc., Logan, UT, USA) and were averaged to 30-min intervals.

Normalized difference vegetation index (NDVI) was used as a proxy to represent the development and growth of the submerged aquatic vegetation. The NDVI data was obtained from the MODIS sensor on NASA's Terra platform. The temporal and spatial resolution of NDVI are 16 days and 250 m, respectively.

The measurement systems were visited every one to two months. The EC gas analyzers were calibrated every year using primary standard CO_2 and CH_4 gases (1% uncertainty) made by the National Institute of Metrology of China and a portable dew point generator (Model LI-610, LI-COR, Inc., Lincoln, NE, USA). The 30-min flux data and micrometeorological data were downloaded weekly by a cellular communication device (Model H7118 GPRS/EDGE DTU, Hongdian Technologies Corporation, Shenzhen, China). The 10 Hz raw EC data were retrieved on site visits.

2.3. Data processing

2.3.1. CH_4 flux data

We processed the raw time series with the Eddy Pro software (version 6.2.1, LI-COR, Lincoln) to produce 30-min CH_4 flux. The sonic temperature was corrected for humidity effects (Van Dijk et al., 2004). A double coordinate rotation was used to force the average vertical velocity to zero and to align the horizontal wind to the mean wind direction (Baldocchi et al., 2000; Wilczak et al., 2001). Statistical tests were carried out on the high frequency data to remove spikes (Vickers and Mahrt, 1997). The time lag caused by the separation between the anemometer and the CH_4 analyzer was compensated by a covariance maximization procedure (Horst and Lenschow, 2009). The loss of flux in the low and high frequency parts of the spectrum was compensated by the methods of Moncrieff et al. (1997, 2004). The Webb-Pearman-Leuning (WPL) correction was applied to remove the density effects of temperature and water vapor variations on the measured CH_4 flux (Webb et al., 1980).

The 0–1-2 system (Mauder and Foken, 2004) was used for the CH_4 flux data quality control. The data flagged by 0 and 1 represent measurements whose 10 Hz time series of w' and c' satisfy the stationarity criterion. According to Mauder and Foken (2004), random flux errors are minimal if this criterion is met. The flux data with quality flag 2 does not satisfy stationarity and was excluded from further analysis. The percent of valid half-hourly CH_4 data was 38% from May 2014 to May 2017. The remaining gaps (62%) were mostly caused by instrument problems (power failure, dirty optical window, and rain interference). No gap-filling was applied at half-hourly intervals. Daily and monthly CH_4 flux were calculated on the basis of the valid half-hourly data. If the valid flux data exceeded 20% in a month, a diurnal composite flux variation was calculated for that month. A daily mean flux was calculated if there were 30% or more valid 30-min data in that day. The percent of valid daily data was 50%. A monthly average flux was produced if the valid 30-min flux data exceeded 20% in that month. These daily and monthly flux calculation criteria were a compromise between adequate temporal coverage and robustness of the daily and month mean fluxes. Use of gap-filled data resulted in essentially the same annual flux (Section 4.3) The flux relationships with environmental factors were investigated at half-hourly and daily time scales.

2.4. CO_2 flux data

We used the CO_2 flux measured with EC to understand the relationship between the CH_4 flux and the net ecosystem production. The CO_2 flux data was processed using the same procedure as the CH_4 flux, with the following additional steps. In addition to the standard WPL correction, a small correction was applied to the CO_2 flux to remove the spectroscopic effect caused by the slow response of the temperature sensor integrated in the EC gas analyzer (Bogoev, 2014; Wang et al., 2016). Abnormal CO_2 flux data was filtered according to the following conditions, (1) when precipitation happened, (2) when the flux was lower than -1.5 mg m^{-2} s^{-1} or >1.5 mg m^{-2} s^{-1}, and (3) when the standard deviation of CO_2 concentration was larger than 20 mg m^{-3}.

After data quality control, the valid half-hourly CO_2 data was about 77% from 2014 to 2017. Gaps in the CO_2 flux data were filled with a lookup table. The table was created based on monthly periods. A diurnal composite data table was calculated for every month using the valid 30-min flux. The missing data in a certain half-hour was filled with the data in the corresponding half-hour of the table. The monthly and annual fluxes were calculated using the filled continuous 30-min CO_2 flux data time series. Additional information on the CO_2 flux data processing and interpretation can be found in Lee et al. (2018) (manuscript submitted). An implicit assumption is that the monthly and annual CO_2 flux measured above the water column represents the true NEP of the submerged aquatic habitat. The net water transport of dissolved organic and inorganic carbon into and out of the local domain was omitted. (At the monthly and annual time scales, changes in the CO_2 concentration in the water column are negligible.)

2.5. Modeling turbulent diffusion coefficient of water

Lake CH_4 flux is affected by water turbulence (Podgrajsek et al., 2014). We used the one-dimensional k-ε model developed by Herb and Stefan (2005) to characterize turbulent motion in the lake. The model calculates the budget of the turbulent kinetic energy (TKE) from wind-driven turbulence, density gradient, and dissipation by

macrophytes, and uses the predicted TKE to parameterize the turbulent diffusion coefficient K in the one-dimensional heat diffusion equation. We forced the model using the observed meteorological variables (incoming solar and longwave radiation, wind speed, air temperature and humidity). The important parameters included light extinction coefficient of water (2 m^{-1}), light extinction coefficient of the submerged vegetation (0.02 m^2 gdw^{-1}), the depth of water (2 m), the height of submerged vegetation (1.2 m), and the maximum biomass density (300 gdw m^{-3}). Its lower boundary condition was the measured sediment temperature at the 3-cm depth below the water column. The vertical turbulent diffusion coefficient at the 20-cm depth of the water column simulated by the model was used to investigate the effect of water turbulence on the observed CH_4 flux.

3. Results

3.1. Temporal variations of meteorological factors

The general meteorological conditions experienced in this experiment are shown in a series of averaged diurnal variations, including net radiation (R_n), air temperature (T_a), 20-cm depth water temperature (T_w), sediment temperature (T_s) and wind speed (WS) for each of the four seasons (spring, from March to May; summer, from June to August; autumn, from September to November; winter, from December to February in next year; Supplementary Fig. S1 and Fig. S2). The midday seasonal mean R_n varied from 325 W m^{-2} (winter) to 515 W m^{-2} (summer). The highest T_a and T_w occurred in the afternoon, at about 16:00 local time (Fig. S1), with seasonal mean midafternoon values of 8.0 and 8.0 °C in the winter and 28.4 and 28.7 °C in the summer, respectively. The sediment temperature (T_s) did not show diurnal variations, was on average 0.5 °C higher than T_w in the winter and 1.9 °C lower than T_w in the summer (Fig. S1). Wind speed (WS) was generally higher in the nighttime than that in the daytime (Fig. S2). The diurnal variation in WS was largest in the summer, showing the seasonal mean peak value of 4.8 m s^{-1} at 21:00, and mean minimum value of 3.7 m s^{-1} at 12:00. The diurnal variations of turbulent diffuse coefficient at the 20-cm water depth (K) were similar to the patterns for WS. In the summer, the seasonal mean peak value of 12.9 cm^2 s^{-1} occurred at 23:00 and mean minimum value of 6.9 cm^2 s^{-1} at 12:30 (Fig. S2). The monthly mean T_a reached a maximum of 28.0 °C in July, and the monthly mean T_w and T_s were the highest, at 29.0 and 27.8 °C, respectively, in August (Supplementary Fig. S4).

3.2. Temporal variations of the CH_4 flux

According to all valid 30-min and 5-day mean CH_4 flux from DOY (day of year) 121 (May 1st), 2014 to DOY 150 (May 30), 2017, the flux was higher in the summer and the autumn (June to November, mean value 0.33 μg CH_4 m^{-2} s^{-1}) and lower in the winter and the spring (December to May in next year, mean value 0.18 μg CH_4 m^{-2} s^{-1}; Fig. S5).

In general, CH_4 flux was lower in the daytime than at night (Table 1). The mean nighttime flux was 43%, 29%, 25%, and 36% higher than the mean daytime flux in the spring, summer, autumn, and winter, respectively. Averaged over the four seasons, the nighttime flux was 33% ± 8% higher than the daytime flux. However, large fluxes were often observed in the daytime, resulting in scatters in the diurnal flux composites, except in the spring when a clear diurnal pattern was evident (Fig. 2).

Clear season variations in the flux are shown by the monthly values (Fig. 3). Eight of the monthly values were averages of at least two monthly data from different years, and the remaining monthly values were based on data collected in one year only. The lowest monthly mean was 0.14 ± 0.001 μg CH_4 m^{-2} s^{-1} in February, and the highest was 0.49 ± 0.03 μg CH_4 m^{-2} s^{-1} in August. The annual mean flux based on the 12 monthly mean values shown in Fig. 3 was 0.26 ± 0.10 μg CH_4 m^{-2} s^{-1}, corresponding to an annual total of 6.12 ± 0.11 g C m^{-2} yr^{-1}.

Table 1
CH_4 flux in daytime and nighttime in the four seasons (Unit: μg CH_4 m^{-2} s^{-1}). The range of variation is ± one standard deviation.

	Spring	Summer	Autumn	Winter
Daytime[a]	0.14 ± 0.05	0.33 ± 0.10	0.23 ± 0.07	0.14 ± 0.07
Nighttime[b]	0.25 ± 0.12	0.47 ± 0.11	0.31 ± 0.10	0.22 ± 0.08

[a]Solar elevation angle is higher than 25°.
[b]Solar elevation angle is lower than −25°.

3.3. Effects of environmental factors on the CH_4 flux

To probe the mechanisms that drove the diurnal flux variations, we first computed the mean values of the flux and meteorological variables for each 30-min period of the day and correlated the 30-min flux with the 30-min meteorological variables. We found positive and significant correlation between the flux with wind speed WS and the turbulent diffusion coefficient K in the summer (Fig. 4a and b) and in the other three seasons (Supplementary Fig. S6). Moreover, F_m showed significant relationship with sediment temperature in the summer only and did not show significant relationship with air pressure in any of the four seasons.

The daily mean flux increased exponentially with sediment temperature T_s (Fig. 4c), resulting in a Q_{10} value of 1.79. The exponential fit function explains 71% (or R^2 of 0.71) of the observed flux variations. Here the daily data were first grouped into 1 °C bins and the regression was applied to the bin-averaged flux. If the water temperature instead of the sediment temperature was used as independent variable in this regression, the coefficient of determination would be slightly lower at $R^2 = 0.63$, indicating that sediment temperature exerted a stronger control than water temperature on methane production at this habitat of submerged aquatic vegetation.

The temperature response here (at BFG) contrasted sharply with that observed at Meiliangwan (Site ID MLW, Fig. 1), a site located in the eutrophic zone in the northern part of the lake, with the latter showing a threshold instead of a continuous pattern (Fig. 4c). Below the temperature of 23 °C, the flux at MLW was insensitive to temperature. When the sediment temperature was higher than 23 °C, the flux at MLW increased rapidly with temperature. Forcing a regression fit with an exponential function resulted in an unrealistically high Q_{10} of 239 at MLW.

The daily mean flux at BFG also showed a weak negative but significant correlation with air pressure (P) (Fig. 4d).

A stepwise multiple linear regression was applied to the monthly data, with the monthly flux F_m as the dependent variable and the monthly mean T_w, T_s, P, and NDVI as the independent variables. The final regression model is $F_m = (0.011 \pm 0.002)\ T_s + (0.073 \pm 0.041)$ ($R^2 = 0.50$, $p < 0.01$). The result shows that the monthly mean T_s was the best predictor for F_m.

3.4. Relationship between the CH_4 flux and the net ecosystem productivity

When presented in a scatter plot, the monthly mean methane flux is uncorrelated with the monthly NEP (Fig. 5a). The ratio of the monthly mean CH_4 flux to the monthly mean CO_2 flux or NEP is given in Fig. 5b. Both fluxes are expressed in g C m^{-2} s^{-1}. This flux ratio varied between a low value of −0.4% in November to a maximum value of 12.3% in December, with both showing large inter-annual variability (standard deviation 6.4 to 14.9%), because the NEP fluctuated greatly in these two months. If these two months were excluded, the flux ratio was higher in the warm season (5.9%, June to September) than in the cold season (2.5%, January to May and October).

At the annual scale, the methane flux was 6.57 g C m^{-2} yr^{-1} and 6.37 g C m^{-2} yr^{-1} in 2015 and 2016, respectively, based on the mean

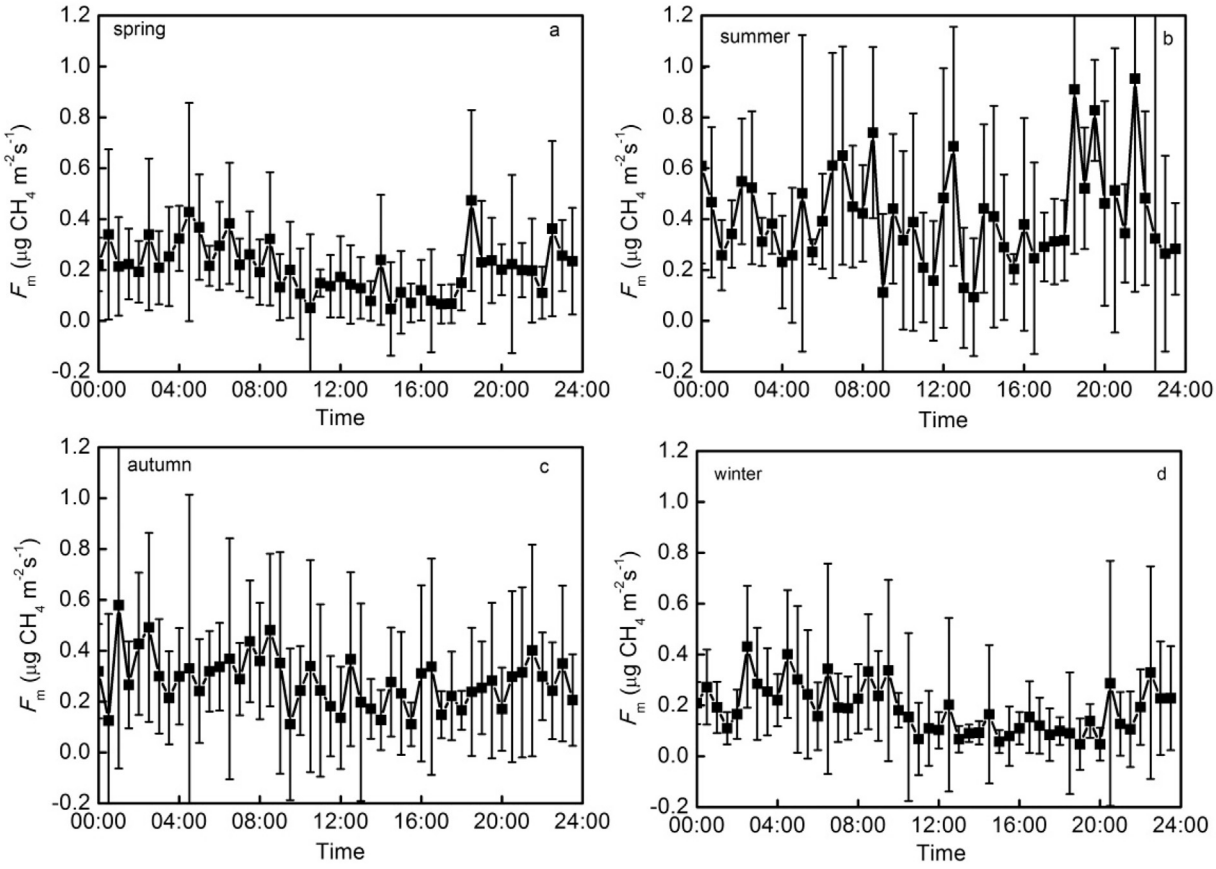

Fig. 2. Average diurnal composite CH_4 flux (F_m) at BFG in the spring (a), summer (b), autumn (c), and winter (d) from 2014 to 2017 at BFG. Error bars are ± one standard deviation.

value of valid daily flux data without gap-filling. In comparison, the annual NEP was 165 g C m^{-2} $yr^{-1}$and 215 g C m^{-2} yr^{-1} in 2015 and 2016, respectively. On average, about 3.5% of the carbon taken up from the atmosphere by the submerged vegetation was lost in the form of methane to the atmosphere.

4. Discussion

4.1. Diurnal variations of the CH_4 flux in wetlands and lakes

Four processes, plant transport, production, diffusion and oxidation, can potentially result in diurnal changes in the methane flux. In some wetlands, eddy covariance observations show higher CH_4 flux values in the daytime than at night (Matthes et al., 2014; Koebsch et al., 2015; van den Berg et al., 2016). This is because the plant-mediated transport is the main pathway of CH_4 emission in ecosystems with emergent vascular vegetation whose stomata remain open in the daytime (Miller, 2011; Bhullar et al., 2013; Knoblauch et al., 2015). In this study, the generally higher CH_4 flux at night than during the day (Table 1) does not support the plant-mediated transport mechanism. Furthermore, our observed diurnal pattern cannot be explained by changes in methane production in the sediment because the diurnal amplitude of the sediment temperature was negligible (Supplementary Fig. S1). If we used the 20-cm water temperature as a predictor for the half-hourly bin averaged flux, the regression equation is $y = (0.151 \pm 0.033)\, e^{(0.032\pm0.081)\,x}$ ($R^2 = 0.58$), where y is in μg CH_4 m^{-2} s^{-1} and x is in °C. Given a typical seasonal mean T_w diurnal amplitude of 1.6 °C (Supplementary Fig. S1), this equation predicts a diurnal change in the methane flux of 0.014 μg CH_4 m^{-2} s^{-1}, still too small in comparison to the observed difference between daytime and nighttime (average difference 0.1 μg CH_4 m^{-2} s^{-1}).

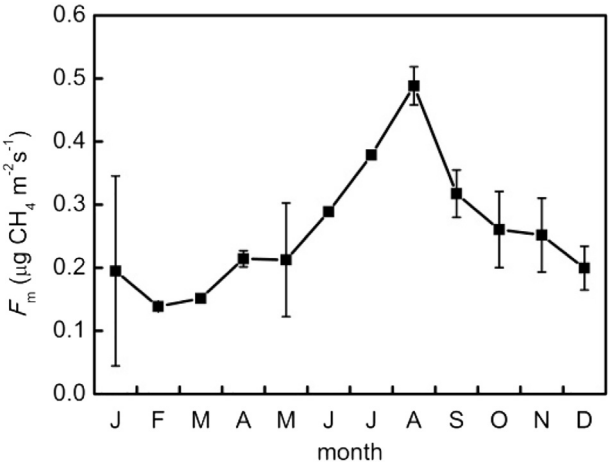

Fig. 3. Monthly CH_4 flux (F_m) from May 2014 to May 2017 at BFG. Error bars are ± one standard deviation of average monthly values.

Diurnal patterns of higher nighttime flux have also been reported for shallow lakes and ponds with (Podgrajsek et al., 2014) and without submerged vegetation (Godwin et al., 2013; Franz et al., 2016). A potential mechanism is that water-side convection triggered by cold surface water at night promotes diffusion of methane out of the water column (Podgrajsek et al., 2014). In the present study, the same mechanism was a more logical explanation for the diurnal flux pattern than changes in methane production because of the higher eddy diffusion coefficient K at night than during the day (Fig. S2). A contributor to the higher K at night was higher wind speed at night than during the day (Fig. S2). Additionally, the water column was generally well mixed at night due to convection but was stably stratified during the day (Fig. S3). Mixing of the water column at night can bring methane-rich water near the sediment to the surface, enhancing the flux to the atmosphere. Moreover,

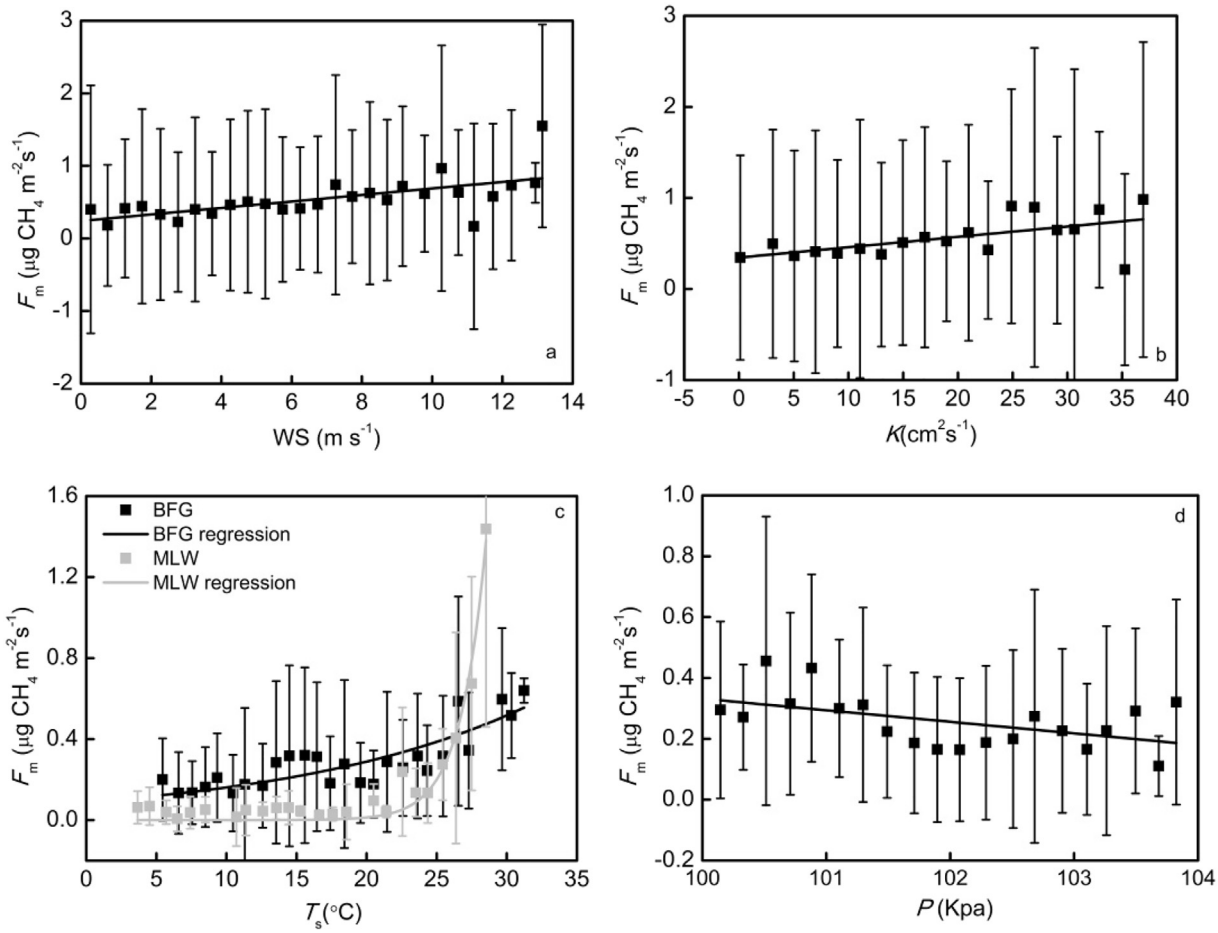

Fig. 4. Relationships between CH_4 flux (F_m) and environmental variables: (a) relationship of half-hourly bin average flux with wind speed (WS) at BFG in the summer; (b) relationship of half-hourly bin average flux with turbulent diffusion coefficient at the 20-cm water depth (K) at BFG in the summer; (c) bin average daily flux and sediment temperature (T_s) at BFG and MLW; (d) bin-average daily flux and air pressure (P) at BFG. The regression statistics are: $y = (0.045 \pm 0.011)x + (0.241 \pm 0.081)$, $R^2 = 0.42$, $p < 0.01$ in panel (a), $y = (0.011 \pm 0.003)x + (0.344 \pm 0.083)$, $R^2 = 0.35$, $p < 0.01$ in panel (b), BFG: $y = (0.090 \pm 0.018)\, e^{(0.058 \pm 0.008)x}$, $R^2 = 0.71$, $p < 0.01$; MLW: $y = (2.256 \times 10^{-7} \pm 2.779 \times 10^{-7})\, e^{(0.548 \pm 0.044)x}$, $R^2 = 0.96$, $p < 0.01$ in panel (c), and $y = (-0.038 \pm 0.015)x + (4.131 \pm 1.579)$, $R^2 = 0.25$, $p < 0.05$ in panel (d). All parameter bounds on the regression coefficients are 95% confidence intervals.

strong water turbulence generated by convection and wind shear can promote bubble CH_4 emission from the sediment in shallow lakes (Mattson and Likens, 1990; Podgrajsek et al., 2014). It is suggested that water turbulence can promote bubble formation at the water-sediment interface (Joyce and Jewell, 2003; Podgrajsek et al., 2014).

Finally, the day versus night contrast may be related to oxygen levels in the water and the sediment. During the day, submerged macrophytes can transport oxygen to the root zone (Sorrell et al., 2002; Sorrell and Downes, 2004; Xing et al., 2006), supporting methanotrophs and other organisms that consume methane. During photosynthesis, oxygen is released by the foliage layer, potentially increasing the oxidation rate of methane during the process of diffusion through the water column. At night, the environment is more anoxic, and methane can diffuse out of the sediment and the water column more readily. In this regard, the diurnal CH_4 flux phenomenon is similar to the diurnal variations in hydrogen sulfide release from sediment (Lee and Dunton, 2000; Hebert and Morse, 2003; Hebert et al., 2007).

4.2. Temperature sensitivity of the CH_4 flux

In general, the lake CH_4 flux increases exponentially with water or sediment temperature (Kankaala et al., 2004; Duan et al., 2005; Xing et al., 2005; Koebsch et al., 2015; Franz et al., 2016; Liu et al., 2017). This temperature dependence was evident at daily time scales (Fig. 4c) and also explained the observed seasonal variations (Fig. 3) at Lake Taihu. This temperature relationship results from higher activity of methaneogenic bacteria and higher methane production at higher temperatures (Kankaala et al., 2004; Song et al., 2013; Yvon-Durocher et al., 2014).

The Q_{10} parameter is a quantitative measure of the temperature sensitivity. Table 2 is a summary of the Q_{10} values found for lakes and wetlands in the published literature. In this study, the Q_{10} value was 1.79 for the submerged aquatic vegetation zone. This value was close to the value observed for Lake Poyang, another subtropical lake but without aquatic vegetation, was generally lower than the values reported for wetlands (2.0 to 5.6) and for temperate and boreal lakes with or without aquatic vegetation (3.2 to 22.9). According to the incubation experiments of soil samples collected from wetland and paddy ecosystems, the range of Q_{10} of potential methane production is from 1.5 to 28 (Segers, 1998). Our relatively low Q_{10} value for the submerged aquatic habitat may be related to the warm climate and the relative long growing season in the Yangtze River Delta. At Lake Taihu, the annual mean air temperature was 16.2 °C. The growing season of submerged vegetation is from March to November according to field surveys by Luo et al. (2017). Our EC measurement indicates that the monthly mean CO_2 flux was negative throughout the year, indicating photosynthetic activity even in the winter (Lee et al., 2018; manuscript in review). Active primary production in the cold season, coupled with the death of some biomass, may have enhanced substrate supply for methanogenesis, thus offsetting the cold temperature effect. In January 2016, the coldest month (mean air temperature 4 °C) at Lake Taihu, the CH_4 flux was 0.30 μg CH_4 m^{-2}, which is actually higher than the flux (0.07 μg CH_4 m^{-2}) observed in rice paddies during the seeding period (from April to May) in California (McMillan et al., 2007).

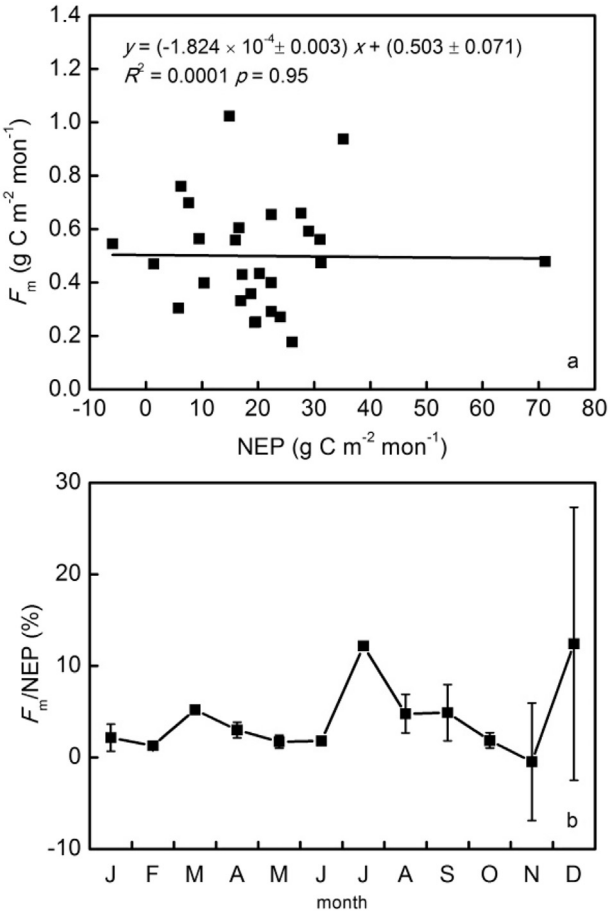

Fig. 5. Relationship between methane and carbon fluxes at BFG. (a) Scatter plot of the monthly mean methane flux versus monthly NEP. (b) The ratio of monthly carbon lost via CH_4 emission (F_m) to the carbon gained via net primary productivity (NEP). Error bars are ± one standard deviation. Also shown in panel (a) are regression statistics.

In comparison, the overall Q_{10} value was 239 for the MLW site located in the highly eutrophic zone of the lake where algal growth was common in high temperatures. We suggest that this site experienced two different states. When the sediment temperature was lower than 23 °C, the CH_4 flux was low (Fig. 10b) and presumably originated from the decomposition of organic matter in the sediment. The average flux for temperatures lower than 23 °C was 0.04 μg CH_4 m^{-2} s^{-1}. When the sediment temperature was higher than 23 °C, the CH_4 flux became much higher (average value 0.47 μg CH_4 m^{-2} s^{-1}), which was indicative of more efficient methane production from dead algal biomass, and showed a rapid increase with increasing temperature. If we restricted the regression fit to the data with temperatures higher than 23 °C, we obtained a more reasonable Q_{10} value of 33.1. The unusually high overall Q_{10} was an artifact of the regression fit to two different methane production regimes. Nevertheless, the threshold behavior of the methane flux suggests a higher temperature sensitivity of the flux for eutrophic waters than for more clean waters.

4.3. Comparison of annual CH_4 emission

The annual CH_4 flux value reported here (6.12 g C m^{-2} yr^{-1}) for the submerged aquatic vegetation habitat of Lake Taihu is near the high end of the flux values reported previously for Lake Taihu and other subtropical lakes in China. In a study of methane spatial variations across Lake Taihu, Xiao et al. (2017) found the highest dissolved methane concentration in the zone of submerged macrophytes. Using the piston velocity method and sampling of CH_4 dissolved in water, they show large spatial variations of the diffusion CH_4 flux are controlled primarily by water quality and vegetation type across the lake. By combining the diffusion flux and an estimate of the ebullition contribution, they estimated that the total whole-lake mean CH_4 flux is 1.15 g C m^{-2} yr^{-1}. Using the flux-gradient technique, Xiao et al. (2014) reported an annual flux of 1.35 g C m^{-2} yr^{-1} for the eutrophic phytoplankton zone in the northern portion of Lake Taihu. Wang et al. (2006) deployed the chamber method in an infralittoral zone in the northern portion of Lake Taihu, yielding an annual flux of 2.62 g C m^{-2} yr^{-1}. Our annual flux is close the flux value of 6.36 g C m^{-2} yr^{-1} reported for Lake Donghu (Xing et al., 2005) but is much higher than the flux value of 2.38 g C m^{-2} yr^{-1} for Lake Poyang (Liu et al., 2017). Like Lake Taihu, Lake Donghu is a shallow lake, with a mean water depth of 2.5 m, but is hypereutrophic and dominated by phytoplankton. On the other hand, Lake Poyang is much deeper (mean depth of 8 m).

The annual lake CH_4 flux varies by climate. According to Bastviken et al. (2011), the global flux from open waters on land is about 14 g C m^{-2} yr^{-1}, which is much lower than the flux of 34 g CH_4 m^{-2} yr^{-1} for lakes in the tropical zone (latitude <24°) (Bastviken et al., 2011). The annual CH_4 emission from the submerged aquatic vegetation zone of Lake Taihu is lower than the global level and much lower than the CH_4 emission from lakes in the tropical climate. Many of the lakes located in the temperate climate surveyed by Bastviken et al. (2004) are surrounded by bogs and forests which provide large quantities of organic carbon as input into these lakes, thus supporting high methane emissions. The tropical lakes in Bastviken et al. (2004) are mostly located in floodplains where primary productivity is large, temperature is high, and flood water is shallow (Crill et al., 1988; Devol et al. 1988 & 1990; Engle and Melack, 2000; Smith et al., 2000; Bastviken et al., 2010). These conditions favor high methane fluxes. For example, the CH_4 flux is 38 g CH_4 m^{-2} yr^{-1} in lakes near Pantanal, in a

Table 2
Temperature sensitivity of methane flux (Q_{10}) for different inland water ecosystems.

Ecosystem type	Climate zone	Vegetation type	Temperature	Q_{10}	Reference
Lake	Subtropical	Submerged	Sediment	1.8	This study
Lake	Subtropical	Algal	Sediment	239	This study
Lake	Boreal	Emergent	Sediment	3.2–6.0	Kankaala et al., 2004
Boreal lakes	Boreal	–	Water	15.8	Rasilo et al., 2015
Lake	Temperate	Submerged and floating	Soil	22.9	Franz et al., 2016
Lake	Temperate	Emergent	Sediment	3.2–5.1	Duan et al., 2005
Lake	Subtropical	–	sediment	1.7–2.0	Liu et al., 2017
Wetland	Temperate	Emergent	Soil/water	2.7	Bansal et al., 2016
Wetland	Boreal	Emergent	Soil	2.2–2.6	Sun et al., 2018
Wetland	Boreal	Emergent	Soil	5.6	Gill et al., 2017
Wetland	Subtropical	Emergent	Soil	3.4–3.8	Wang et al., 2015
Wetland	Temperate	Emergent	Air	2.6–3.7	Boardman et al., 2013
Wetland	Alpine	Emergent	Soil	2.4	Song et al., 2015
Peatland	Boreal	Emergent	Soil	2.0	Pypker et al., 2013
Wetland	Boreal	Emergent	Soil	4.4	Herbst et al., 2011

savannah floodplain in South American (Marani and Alvalá, 2007; Bastviken et al., 2010).

Methodological differences are a confounding factor in the above flux comparison. For example, micrometeorological methods measure the total flux (ebullition plus diffusion) whereas the water equilibrium method only measures the diffusion flux (Schubert et al., 2012). In this regard, the comparison between BFG and MLW is noteworthy because the measurement was made at the same time and the techniques – eddy covariance at BFG and flux-gradient at MLW – both measured the total flux with similar footprint sizes. These two sites experienced similar wind speeds (annual mean 3.5 m s^{-1} at MLW and 4.5 m s^{-1} at BFG) and nearly identical water temperature and solar radiation (Wang et al., 2014; Xiao et al., 2017). But TP, TN and chlorophyll-a concentrations were much higher at MLW in the eutrophic phytoplankton zone than at BFG in the submerged aquatic vegetation zone (Xiao et al., 2017). The flux at MLW was much lower than at BFG except during a brief period when daily mean temperature rose above 23 °C (Fig. 4c). Because of the highly non-linear flux behavior with respect to sediment temperature and large data gaps (daily flux gap 70%) at MLW, we could not obtain a reliable gap-filled annual flux for the observational period. A previous study using the same flux-gradient system reported an annual flux of 1.35 g C m^{-2} yr^{-1} for MLW.

Another confounding factor is related to data gaps. The annual CH_4 emission total reported above for BFG (6.12 g C m^{-2} yr^{-1}) was based on the simple algebraic mean flux without regard to data gaps. Using the regression equation in Fig. 4c to fill data gaps, we obtained a slightly larger annual total of 6.48 ± 0.16 g C m^{-2} yr^{-1}. Here, the uncertainty range is ±1 standard deviation of 10,000 ensemble members of a Monte Carlo simulation assuming that errors in the regression coefficient follow a normal distribution. In other words, our general findings seem robust and unaffected by data gaps.

4.4. Relation of annual methane flux to net ecosystem production

An important driver of the annual CH_4 flux is primary production. In the submerged aquatic vegetation zones in a temperate fen and in a Mediterranean wetland, the CH_4 flux is 39.5 and 104 g C m^{-2} yr^{-1}, respectively (Franz et al., 2016; Miller, 2011). These values are much higher than the CH_4 emission flux from this study, largely because of higher NEP at those sites than at BFG. Although no NEP data have been reported for the temperate fen, the NEP is about 800 g C m^{-2} yr^{-1} for the Mediterranean wetland (Miller, 2011), or 4 times the NEP of our site (190.2 g C m^{-2} yr^{-1}). Xing et al. (2006) reported that the CH_4 emission flux is 6.6 g C m^{-2} yr^{-1} and the net primary productivity (NPP) is 120 to 150 g C m^{-2} yr^{-1} for a submerged aquatic vegetation habitat of Lake Biandantang in an alluvial plain in the middle of the Yangtze River. These flux values were similar to ours.

Table 3 is a summary of the ratio of the amount of carbon lost via CH_4 emission to the amount of carbon gained through photosynthesis, expressed as NEP, NPP or gross primary productivity (GPP), found in the published literature. In wetlands with emergent vegetation, the ratio of methane flux to NEP varies from 1.1% to 16.3%, with a mean of 7.3%. For rice paddies, the ratio is in the range of 3.5% to 5.6%. For comparison, the ratio of CH_4 emission to NEP was 3.5% at the annual scale for our study site, which is close to the mean ratio of 3.3% for wetland and rice ecosystems (Whiting and Chanton, 1993). These broadly similar ratios suggest that BFG behaved more like wetland systems than open-water systems. Future research should test if NEP-based CH_4 models for wetland ecosystems can be applied to submerged aquatic vegetation habitats.

5. Conclusions

At BFG, a submerged macrophyte habitat in Lake Taihu, the eddy covariance measurement showed that the CH_4 flux was higher at night than during the day. Possible drivers of this diurnal pattern included changes in the diffusion efficiency of the water column and oxygen levels between day and night. At the seasonal time scale, the sediment temperature was the primary driver of the CH_4 flux variations, implying higher methane production in the sediment at higher temperatures.

The sensitivity of the CH_4 flux to sediment temperature was low (Q_{10} = 1.79), because active primary production, coupled with the death of some biomass in the cold season, may have enhanced substrate supply for methanogenesis, thus offsetting the cold temperature effect. In contrast, the Q_{10} value for MLW, a site in the eutrophic phytoplankton zone in the northern portion of Lake Taihu, was 239. We suggest that the unusually high overall Q_{10} at MLW was an artifact of forcing the regression fit of the exponential function to two different methane production regimes.

The annual CH_4 emission was 6.12 g Ccm^{-2} yr^{-1} at BFG, which is much higher than that reported previously by Xiao et al. (2014) (1.35 g C m^{-2} yr^{-1}) for MLW in the eutrophic phytoplankton zone. On the monthly time scale, the CH_4 flux and the NEP were uncorrelated. On the annual time scale, the ratio of the CH_4 flux to NEP was about 3.5%, similar to the ratios reported previously for natural wetlands and rice paddies.

Table 3
The ratio of carbon lost via CH_4 emission to the carbon gained through photosynthesis for different freshwater ecosystems.

Ecosystem type	Vegetation type	Climate	Ratio	References
Rice paddy	Rice	Mediterranean	3.5%[a]	Knox et al., 2016
Rice paddy	Rice	Temperate	4.8–5.6%[a]	McMillan et al., 2007
Freshwater marsh	EV[e]	Subtropical	14.0%[a]	Krauss et al., 2016
Marsh	EV[e]	Subtropical	1.1%[a]	Whiting et al., 1991
Peatland	EV[e]	Boreal	2.9%[a]	Whiting and Chanton, 1992
Bogs and Fens	EV[e]	Boreal	7.5%[c]	Crill et al., 1988
Swamp	EV[e]	Temperate	3.5%[a]	Chanton et al., 1992
Tundra	EV[e]	Boreal	6%[a]	Fan et al., 1992
Wetland	EV[e]	Temperate	2.6%[a]	Morin et al., 2014
Fen	Small EV[e]	Temperate	7.9–10.9%[a]	Minke et al., 2016
Fen	Tall EV[e]	Temperate	8.5–16.3%[a]	Minke et al., 2016
Bog	EV[e]	Temperate	1.5%[a]	Wilson et al., 2013
Wetland	EV[e]	Temperate	8.7%[a]	Brix et al., 2001
Fen	EV[e]	Temperate	9.5–14.4%[a]	Knox et al., 2015
Fen	EV[e]	Boreal	2.3%[a]	Ström et al., 2015
Wetland	SAV[d]	Mediterranean	11.7%[a]	Miller, 2011
Fen	SAV[d]	Temperate	14.0%[b]	Franz et al., 2016
Lake	SAV[d]	Subtropical	0.7–1.4%[c]	Xing et al., 2006
Lake	Phytoplankton	Subtropical	15.3%[c]	Xing et al., 2005
Lake	SAV[d]	Subtropical	3.5%[a]	This study

[a]The ratio of CH_4 emission (g C m^{-2} yr^{-1}) to NEP (g C m^{-2} yr^{-1}).
[b]The ratio of CH_4 emission (g C m^{-2} yr^{-1}) to GPP (g C m^{-2} yr^{-1}).
[c]The ratio of CH_4 emission (g C m^{-2} yr^{-1}) to NPP (g C m^{-2} yr^{-1}).
[d]Submerged aquatic vegetation.
[e]Emergent vegetation.

Acknowledgement

This research was supported jointly by the National Natural Science Foundation of China (grant numbers 41575147, 41801093, and 41475141), the Ministry of Education of China (grant number PCSIRT), and the Priority Academic Program Development of Jiangsu Higher Education Institutions (grant number PAPD). We thank all students in Yale-NUIST Center on Atmospheric Environment for their hard work.

Appendix A. Supplementary data

Supplementary data to this article can be found online at https://doi.org/10.1016/j.scitotenv.2019.03.466.

References

Baldocchi, D., Finnigan, J., Wilson, K., Paw, U.K.T., Falge, E., 2000. On measuring net ecosystem carbon exchange over tall vegetation on complex terrain. Bound.-Layer Meteorol. 96, 257–291.

Bansal, S., Tangen, B., Finocchiaro, R., 2016. Temperature and hydrology affect methane emissions from prairie pothole wetlands. Wetlands 36 (Suppl. 2), S371–S381.

Bastviken, D., Cole, J., Pace, M., Tranvik, L., 2004. Methane emissions from lakes: dependence of lake characteristics, two regional assessments, and a global estimate. Glob. Biogeochem. Cycles 18, 1–12.

Bastviken, D., Santoro, A.L., Marotta, H., Pinho, L.Q., Calheiros, D.F., Crill, P., Enrich-Prast, A., 2010. Methane emissions from Pantanal, South America, during the low water season: toward more comprehensive sampling. Environ. Sci. Technol. 44, 5450–5455.

Bastviken, D., Tranvik, L.J., Downing, J.A., Crill, P.M., Enrich-Prast, A., 2011. Freshwater methane emission offset the continental carbon sink. Science 331, 50.

Bhullar, G.S., Edward, P.J., Venterink, H.O., 2013. Variation in the plant-mediated methane transport and its importance for methane emission from intact wetland peat mesocosms. J. Plant Ecol. 6 (4), 298–304.

Boardman, C.P., Gauci, V., Fox, A., Blake, S., Beerling, D.J., 2013. Reduction of the temperature sensitivity of minerotrophic fen methane emissions by simulated glacial atmospheric carbon dioxide starvation. J. Geophys. Res. Biogeosci. 118, 462–470.

Bogoev, I., 2014. Improved eddy flux measurements by open-path gas analyzer and sonic anemometer co-location. Geophys. Res. Abstr. 16 Abstract EGU2014–199. [Available online at http://meetingorganizer.copernicus.org/EGU2014/ EGU2014-199.pdf.].

Brix, H., Sorrell, B.K., Lorenzen, B., 2001. Are *Phragmites*-dominated wetlands a net source or net sink of greenhouse gases? Aquat. Bot. 69, 313–324.

Chanton, J.P., Whiting, G.J., Showers, W.J., Crill, P.M., 1992. Methane flux from *Peltandra Virginica*: stable isotope tracing and chamber effects. Glob. Biogeochem. Cycles 6 (1), 15–31.

Crill, P.M., Bartlett, K.B., Wilson, J.O., Sebacher, D.I., Harriss, R.C., Melack, J.M., MacIntyre, S., Lesack, L., 1988. Tropospheric methane from an Amazonian floodplain lake. J. Geophys. Res. Atmos. 93, 1564–1570.

Dalal, R.C., Allen, D.E., Livesley, S.J., Richards, G., 2008. Magnitude and biophysical regulators of methane emission and consumption in the Australian agricultural, forest, and submerged landscapes: a review. Plant Soil 309, 43–76.

Davidson, T.A., Audet, J., Svenning, J., Lauridsen, T.L., Søndergaard, M., Landkildehus, F., Larsen, S.E., Jeppesen, E., 2015. Eutrophication effects on greenhouse gas fluxes from shallow-lake mesocosms override those of climate warming. Glob. Chang. Biol. 21, 4449–4463.

Devol, A.H., Richey, J.E., Clark, W.A., King, S.L., 1988. Methane emissions to the troposphere from the Amazon floodplain. J. Geophys. Res. Atmos. 93, 1583–1592.

Devol, A.H., Richey, J.E., Forsberg, B.R., Martinelli, L.A., 1990. Seasonal dynamics in methane emissions from the Amazon River floodplain to the troposphere. J. Geophys. Res. Atmos. 95, 16417–16426.

Downing, J.A., Prairie, Y.T., Cole, J.J., Duarte, C.M., Tranvik, L.J., Striegl, R.G., McDowell, W.H., Kortelainen, P., Caraco, N.F., Melack, J.M., Middelburg, J.J., 2006. The global abundance and size distribution of lakes, ponds, and impoundments. Limnol. Oceanogr. 51 (5), 2388–2397.

Duan, X.N., Wang, X.K., Mu, Y.J., Ouyang, Z.Y., 2005. Seasonal and diurnal variations in methane emissions from Wuliangsu Lake in arid regions of China. Atmos. Environ. 39, 4479–4487.

Engle, D., Melack, J.M., 2000. Methane emissions from an Amazon floodplain lake: enhanced release during episodic mixing and during falling water. Biogeochemistry 51, 71–90.

Fan, S.M., Wofsy, S.C., Bakwin, P.S., Jacob, D.J., Anderson, S.M., Kebabian, P.L., Mcmanus, J.B., Kolb, C.E., 1992. Micrometeorologica measurements of CH_4 and CO_2 exchange between the atmosphere and subarctic tundra. J. Geophys. Res. Atmos. 97 (D15), 16627–16643.

Franz, D., Koebsch, F., Larmanou, E., Augustin, J., Sachs, T., 2016. High net CO_2 and CH_4 release at a eutrophic shallow lake on a formerly drained fen. Biogeosciences 13, 3051–3070.

Gill, A.L., Glasson, M.A., Yu, R., Finzi, A.C., 2017. Deep peat warming increases surface methane and carbon dioxide emissions in a black spruce-dominated ombrotrophic bog. Glob. Chang. Biol. 23, 5398–5411.

Godwin, C.M., McNamara, P.J., Markfort, C.D., 2013. Evening methane emission pulses from a boreal wetland correspond to convective mixing in hollows. J. Geophys. Res. Biogeosci. 118, 994–1005.

Hebert, A.B., Morse, J.W., 2003. Microscale effects of light on H_2S and Fe^{2+} in vegetated (*Zostera marina*) sediments. Mar. Chem. 81, 1–9.

Hebert, A.B., Morse, J.W., Eldridge, P.M., 2007. Small-scale heterogeneity in the geochemistry of seagrass vegetated and non-vegetated estuarine sediments: causes and consequences. Aquat. Geochem. 13, 19–39.

Herb, W.R., Stefan, H.G., 2005. Dynamics of vertical mixing in a shallow lake with submersed macrophytes. Water Resour. Res. 41, W02023. https://doi.org/10.1029/2003WR002613.

Herbst, M., Friborg, T., Ringgaard, R., Soegaard, H., 2011. Interpreting the variations in atmospheric methane fluxes observed above a restored wetland. Agric. For. Meteorol. 151, 841–853.

Horst, T.W., Lenschow, D.H., 2009. Attenuation of scalar fluxes measured with spatially-displaced sensors. Bound.-Layer Meteorol. 130, 275–300.

Hsieh, C.I., Katul, G., Chi, T., 2000. An approximate analytical model for footprint estimation of scalar fluxes in thermally stratified atmospheric flows. Adv. Water Resour. 23, 765–772.

Joyce, J., Jewell, P.W., 2003. Physical controls on methane ebullition from reservoirs and lakes. Environ. Eng. Geosci. 9 (2), 167–178.

Kankaala, P., Ojala, A., Käki, T., 2004. Temporal and spatial variation in methane emissions from a flooded transgression shore of a boreal lake. Biogeochemistry 68, 297–311.

Knoblauch, C., Spott, O., Evgrafova, S., Kutzbach, L., Pfeiffer, E.M., 2015. Regulation of methane production, oxidation, and emission by vascular plants and bryophytes in ponds of the northeast Siberian polygonal tundra. J. Geophys. Res. Biogeosci. 120, 2525–2541.

Knox, S.H., Sturtevant, C., Matthes, H.J., Koteen, L., Verfaillie, J., Baldocchi, D., 2015. Agricultural peatland restoration: effects of land-use change on greenhouse gas (CO_2 and CH_4) fluxes in the Sacramento-San Joaquin Delta. Glob. Chang. Biol. 21, 750–765.

Knox, S.H., Matthes, J.H., Sturtevant, C., Oikawa, P.Y., Verfaillie, J., Baldocchi, D., 2016. Biophysical controls on interannual variability in ecosystem-scale CO_2 and CH_4 exchange in a California rice paddy. J. Geophys. Res. Biogeosci. 121, 978–1001.

Koebsch, F., Jurasinski, G., Koch, M., Hofmann, J., Glatzel, S., 2015. Controls for multi-scale temporal variation in ecosystem methane exchange during the growing season of a permanently inundated fen. Agric. For. Meteorol. 204, 94–105.

Krauss, K.W., Holm Jr., G.O., Perez, B.C., McWhorter, D.E., Cormier, N., Moss, R.F., Johnson, D.J., Neubauer, S.C., Raynie, R.C., 2016. Component greenhouse gas fluxes and radiative balance from two deltaic marshes in Louisiana: pairing chamber techniques and eddy covariance. J. Geophys. Res. Biogeosci. 121, 1503–1521.

Lee, K.S., Dunton, K.H., 2000. Diurnal changes in pore water sulfide concentrations in *seagrass Thalassia testudinum* beds: the effects of seagrasses on sulfide dynamics. J. Exp. Mar. Biol. Ecol. 25, 201–214.

Lee, X., Liu, S.D., Xiao, W., Wang, W., Gao, Z.Q., Cao, C., Hu, C., Hu, Z.H., Shen, S.H., Wang, Y.W., Wen, X.F., Xiao, Q.T., Xu, J.P., Yang, J.B., Zhang, M., 2014. The Taihu Eddy flux network: an observational program on energy, water and greenhouse gas fluxes of a large freshwater lake. Bull. Am. Meteorol. Soc. 95 (10), 1583–1594.

Lee, X., Zhang, Z., Xiao, W., Gao, Y.Q., Liu, S.D., Wang, W., Wen, X.F., Zhang, M., Cao, C., Huang, W.J., Liu, C., Liu, Q., Hu, C., Hu, Y.B., Pu, Y.N., Xiao, Q.T., Xie, C.Y., Zhao, J.Y., Raymond, P., 2018. Direct flux observation reveals large nighttime uptake of atmospheric carbon by an aquatic ecosystem. J. Geophys. Res. Biogeosci. 2019 (manuscript submitted).

Liu, W., Hu, W., Chen, Y., Gu, X., Hu, Z., Chen, Y., Ji, J., 2007. Temporal and spatial variation of aquatic macrophytes in West Taihu Lake. Acta Ecol. Sin. 27, 159–170.

Liu, L.X., Xu, M., Li, R.Q., Shao, R., 2017. Timescale dependence of environmental controls on methane efflux from Poyang Hu, China. Biogeosciences 14, 2019–2032.

Luo, J.H., Duan, H.T., Ma, R.H., Jin, X.L., Li, F., Hu, W.P., Hu, W.P., Shi, K., Huang, W.J., 2017. Mapping species of submerged aquatic vegetation with multi-seasonal satellite images and considering life history information. Int. J. Appl. Earth Obs. Geoinf. 57, 154–165.

Marani, L., Alvalá, P.C., 2007. Methane emissions from lakes and floodplains in Pantanal, Brazil. Atmos. Environ. 41, 1627–1633.

Matthes, J.H., Sturtevant, C., Verfaillie, J., Knox, S., Baldocchi, D., 2014. Parsing the variability in CH_4 flux at a spatially heterogeneous wetland: integrating multiple eddy covariance towers with high-resolution flux footprint analysis. J. Geophys. Res. Biogeosci. 119, 1322–1339.

Mattson, M.D., Likens, G.E., 1990. Air pressure and methane fluxes. Nature 347, 718–719.

Mauder, M., Foken, T., 2004. Documentation and Instruction Manual of the Eddy Covariance Software Package TK2. University of Bayreuth, Department of Micrometeorology, Arbeitsergebnisse Nr. 26 (42 pp).

McMillan, A.M.S., Goulden, M.L., Tyler, S.C., 2007. Stoichiometry of CH_4 and CO_2 flux in a California rice paddy. J. Geophys. Res. Biogeosci. 112, G01008. https://doi.org/10.1029/2006JG000198.

Miller, R.L., 2011. Carbon gas fluxes in re-established wetlands on organic soils differ relative to plant community and hydrology. Wetlands 31, 1055–1066.

Minke, M., Augustin, J., Burlo, A., Yarmashuk, T., Chuvashova, H., Thiele, A., Freibauer, A., Tikhonov, V., Hoffmann, M., 2016. Water level, vegetation composition, and plant productivity explain greenhouse gas fluxes in temperate cutover fens after inundation. Biogeosciences 13, 3945–3970.

Moncrieff, J.B., Massheder, J.M., Bruin, H.de, Elbers, J., Friborg, T., Heusinkveld, B., Kabat, P., Scott, S., Soegaard, H., Verhoef, A., 1997. A system to measure surface fluxes of momentum, sensible heat, water vapour and carbon dioxide. J. Hydrol. 188–189, 589–611.

Moncrieff, J.B., Clement, R., Finnigan, J., Meyers, T., 2004. Averaging, detrending and filtering of eddy covariance time series. In: Lee, X., Massman, W.J., Law, B.E. (Eds.), Handbook of Micrometeorology: A Guide for Surface Flux Measurements. Kluwer Academic, Dordrecht, pp. 7–31 https://doi.org/10.1007/1-4020-2265-4.

Morin, T.H., Bohrer, G., Frasson, R.P.d.M., Naor-Azreli, L., Mesi, S., Stefanik, K.C., Schäfer, K.V.R., 2014. Environmental drivers of methane fluxes from an urban temperate wetland park. J. Geophys. Res. Biogeosci. 119, 2188–2208.

Nielsen, C.S., Michelsen, A., Strobel, B.W., Wulff, K., Banyasz, I., Elberling, B., 2017. Correlations between substrate availability, dissolved CH4, and CH4 emissions in an arctic wetland subject to warming and plant removal. J. Geophys. Res. Biogeosci. 122, 645–660.

Palma-Silva, C., Marinho, C.C., Albertoni, E.F., Giacomini, L.B., Barros, M.P.F., Furlanetto, L.M., Trindade, C.R.T., de Assis Esteves, F., 2013. Methane emissions in two small shallow neotropical lakes: the role of temperature and trophic level. Atmos. Environ. 81, 373–379.

Podgrajsek, E., Sahlée, E., Rutgersson, A., 2014. Diurnal cycle of lake methane flux. J. Geophys. Res. Biogeosci. 119. https://doi.org/10.1002/2013JG002327.

Pypker, T.G., Moore, P.A., Waddington, J.M., Hribljan, J.A., Chimner, R.C., 2013. Shifting environmental controls on CH_4 fluxes in a sub-boreal peatland. Biogeosciences 10, 7971–7981.

Qin, B.Q., Xu, Q. Wu, Luo, L., Zhang, Y., 2007. Environmental issues of Lake Taihu, China. Hydrobiologia 581, 3–14.

Radomski, P., Perleberg, D., 2012. Application of a versatile aquatic macrophyte integrity index for Minnesota lakes. Ecol. Indic. 20, 252–268.

Rasilo, T., Prairie, Y.T., Del Giorgio, P.A., 2015. Large-Scale Patterns in Summer Diffusive CH_4 Fluxes across Boreal Lakes, and Contribution to Diffusive C Emissions. Global Change Boil. vol. 21 pp. 1124–1139.
Scheffer, M., 2004. Ecology of Shallow Lakes. Springer, Netherlands, pp. 210–288.
Schubert, C.J., Diem, T., Eugster, W., 2012. Methane emissions from a small wind shielded lake determined by eddy covariance, flux chambers, anchored funnels, and boundary model calculations: a comparison. Environ. Sci. Technol. 46 (8), 4515–4522.
Schütz, H., Schröder, P., Rennenberg, H., 1991. Role of plants in regulating the methane flux to the atmosphere. In: Sharkey, T.D., Holland, E.A. (Eds.), Trace Gas Emissions by Plants. Academic Press, San Diego, CA, pp. 29–92.
Segers, R., 1998. Methane production and methane consumption: a review of processes underlying wetland methane fluxes. Biogeochemistry 41, 23–51.
Smith, L.K., Lewis, W.M.J., Chanton, J.P., Cronin, G., Hamilton, S.K., 2000. Methane emissions from the Orinoco River floodplain, Venezuela. Biogeochemistry 51, 113–140.
Song, N., Yan, Z.S., Cai, H.Y., Jiang, H.L., 2013. Effect of temperature on submerged macrophyte litter decomposition within sediments from a large shallow and subtropical freshwater lake. Hydrobiologia 714, 131–144.
Song, W., Wang, H., Wang, G., Chen, L., Jin, Z., Zhuang, Q., He, J.S., 2015. Methane emissions from an alpine wetland on the Tibetan Plateau: neglected but vital contribution of the nongrowing season. J. Geophys. Res. Biogeosci. 120, 1475–1490.
Sorrell, B.K., Downes, M.T., 2004. Water velocity and irradiance effects on internal transport and metabolism of methane in submerged *Isoetes alpinus* and *Potamogeton crispus*. Aquat. Bot. 79, 189–202.
Sorrell, B.K., Downes, M.T., Stanger, C.L., 2002. Methanotrophic bacteria and their activity on submerged aquatic macrophytes. Aquat. Bot. 72, 107–119.
Ström, L., Falk, J.M., Skov, K., Jackowicz-Korczynski, M., Mikhail, M., Christensen, T.R., Lund, M., Schmidt, N.M., 2015. Controls of spatial and temporal variability in CH_4 flux in a high arctic fen over three years. Biogeochemistry 125, 21–35.
Sun, L., Song, C.C., Lafleur, P.M., Miao, Y.Q., Wang, X.W., Gong, C., Qiao, T.H., Yu, X.Y., Tan, W.W., 2018. Wetland-atmosphere methane exchange in Northeast China: a comparison of permafrost peatland and freshwater wetlands. Agric. For. Meteorol. 249, 239–249.
Van den Berg, M., Ingwersen, J., Lamers, M., Streck, T., 2016. The role of *Phragmites* in the CH_4 and CO_2 fluxes in a minerotrophic peatland in southwest Germany. Biogeosciences 13, 6107–6119.
Van Dijk, A., Moene, A.F., De Bruin, H.A.R., 2004. The Principles of Surface Flux Physics: Theory, Practice and Description of the ECPACK Library, Internal Report 2004/1, Meteorology and Air Quality Group, Wageningen University, Wageningen, the Netherlands (99 pp).
Verpoorter, C., Kutser, T., Seekell, D.A., Tranvik, L.J., 2014. A global inventory of lakes based on high-resolution satellite imagery. Geophys. Res. Lett. 41, 6396–6402.
Vickers, D., Mahrt, L., 1997. Quality control and flux sampling problems for tower and aircraft data. J. Atmos. Ocean. Technol. 14, 512–526.
Walter, K.M., Zimov, S.A., Chanton, J.P., Verbyla, D., Chapin III, F.S., 2006. Methane bubbling from Siberian thaw lakes as a positive feedback to climate warming. Nature 443, 71–75.
Walter, K.M., Smith, L.C., Chapin III, F.S., 2007. Methane bubbling from northern lakes: present and future contributions to the global methane budget. Philos. T. R. Soc. A 365, 1657–1676.
Wang, H., Lu, J., Wang, W., Yang, L., Yin, C., 2006. Methane fluxes from the littoral zone of hypereutrophic Taihu Lake, China. J. Geophys. Res. Atmos. 111, D17109. https://doi.org/10.1029/2005JD006864.
Wang, W., Xiao, W., Cao, C., Gao, Z.Q., Hu, Z.H., Liu, S.D., Shen, S.H., Wang, L.L., Xiao, Q.T., Xu, J.P., Yang, D., Lee, X.H., 2014. Temporal and spatial variations in radiation and energy balance across a large freshwater lake in China. J. Hydrol. 511, 811–824.
Wang, C., Lai, D.Y.F., Tong, C., Wang, W., Huang, J., Zeng, C., 2015. Variations in temperature sensitivity (Q_{10}) of CH_4 emission from a subtropical estuarine marsh in southeast China. PLoS One 10 (5), e0125227. https://doi.org/10.1371/journal.pone.0125227.
Wang, W., Xu, J.P., Gao, Y.Q., Bogoev, I., Cui, J., Deng, L., Hu, C., Liu, C., Liu, S.D., Shen, J., Sun, X.M., Xiao, W., Yuan, G.F., Lee, X.H., 2016. Performance evaluation of an integrated open-path eddy covariance system in a cold desert environment. J. Atmos. Ocean. Technol. 33, 2385–2399.
Webb, E.K., Pearman, G.I., Leuning, R., 1980. Correction of flux measurements for density effects due to heat and water vapor transfer. Q. J. R. Meteorol. Soc. 106, 85–100.
Wetzel, R., 2001. Limnology: Lake and River Ecosystems. Academic Press, San Diego, CA, pp. 625–630.
Whiting, G.J., Chanton, J.P., 1992. Plant-dependent CH4 emission in a subarctic Canadian fen. Glob. Biogeochem. Cycles 6 (3), 225–231.
Whiting, G.J., Chanton, J.P., 1993. Primary production control of methane emission from wetlands. Nature 364, 794–795.
Whiting, G.J., Chanton, J.P., Bartlett, D.S., Happell, J.D., 1991. Relationships between CH_4 emission, biomass, and CO_2 exchange in a subtropical grassland. J. Geophys. Res. Atmos. 96 (D7), 13067–13071.
Wilczak, J.M., Oncley, S.P., Stage, S.A., 2001. Sonic anemometer tilt correction algorithms. Bound.-Layer Meteorol. 99, 127–150.
Wilson, D., Farrell, C., Mueller, C., Hepp, S., Wilson, F.R., 2013. Rewetted industrial cutaway peatlands in western Ireland: a prime location for climate change mitigation? Mires Peat 11, 1–22.
Xiao, W., Liu, S.D., Li, H.C., Xiao, Q.T., Wang, W., Hu, Z.H., Hu, C., Gao, Y.Q., Shen, J., Zhao, X.Y., Zhang, M., Lee, X., 2014. A flux-gradient system for simultaneous measurement of the CH_4, CO_2, and H_2O fluxes at a lake−air interface. Environ. Sci. Technol. 48, 14490–14498.
Xiao, Q.T., Zhang, M., Hu, Z.H., Gao, Y.Q., Hu, C., Liu, C., Liu, S.D., Zhang, Z., Zhao, J.Y., Xiao, W., Lee, X., 2017. Spatial variations of methane emission in a large shallow eutrophic lake in subtropical climate. J. Geophys. Res. Biogeosci. 122. https://doi.org/10.1002/2017JG003805.
Xing, Y.P., Xie, P., Yang, H., Ni, L.Y., Wang, Y.S., Rong, K.W., 2005. Methane and carbon dioxide fluxes from a shallow hypereutrophic subtropical lake in China. Atmos. Environ. 39, 5532–5540.
Xing, Y.P., Xie, P., Yang, H., Wu, A.P., Ni, L.Y., 2006. The change of gaseous carbon fluxes following the switch of dominant producers from macrophytes to algae in a shallow subtropical lake of China. Atmos. Environ. 40, 8034–8043.
Yvon-Durocher, G., Allen, A.P., Bastviken, D., Conrad, R., Gudasz, C., St-Pierre, A., Thanh-Duc, N., del Giorgio, P.A., 2014. Methane fluxes show consistent temperature dependence across microbial to ecosystem scales. Nature 507, 488–491.
Zhao, G., Gao, J., Tian, P., Tian, K., Ni, G., 2011. Spatial–temporal characteristics of surface water quality in the Taihu Basin, China. Environ. Earth Sci. 64, 809–819.